Sector Capacity Estimation Based on Differentiated Routes and Busy Levels

Dong Xiangning[1], *Hu minghua*[1*], *Washington Yotto Ochieng*[2]

1. College of Civil Aviation, Nanjing University of Aeronautics and Astronautics, Nanjing 211106, P. R. China;
2. Imperial College London, Centre for Transport Studies, Department of Civil and Environmental Engineering, South Kensington Campus, London SW7 2AZ, United Kingdom

(Received 7 April 2016; revised 27 December 2016; accepted 13 January 2017)

Abstract: Sector capacity estimation plays an important role in applied research of airspace management. Previous researches manifest that sector capacity should be influenced by its standard flow, or routes in that sector. However, if air traffic controller (ATCO) workload busy levels (level of proactivity of an ATCO) are ignored, the estimated sector capacity may not be accurate. There is a need to compare the estimated sector capacity with and without busy levels consideration, both with differentiated routes consideration. This paper proposes a method for sector capacity estimation based on ATCO workload considering differentiated routes and busy levels. Firstly, the main routes in the sector are identified, and for each route, the ATCO workload per flight is determined. Secondly, the workload for each route at three busy levels is determined. Regression analysis is then applied to determine the relationship between workload and the number of flights (with and without considering busy levels) in 15 min and 1 h time slices. Sector capacity is then determined on the basis of a specified workload threshold, for the two cases with and without considering busy levels. Comparing the two scenarios and following validation by ATCO survey, it is found that capacity estimation considering busy levels is a more realistic and accurate approach. The validated capacity values for the Zhengzhou approach (ZHCC AP) airspace sector accounting for the busy levels were determined accurately as 10 and 33 flights for the 15 min and 1 h slices, respectively. The corresponding results without considering busy levels were 12 and 41 flights for the 15 min and 1 h time slices, respectively.

Key words: ATCO workload; airspace sector capacity estimation; differentiated routes; differentiated busy levels

CLC number: V355; U8 **Document code**: A **Article ID**: 1005-1120(2017)04-0438-11

0 Introduction

As the air traffic volume continually increases, it is necessary to divide the airspace into smaller sectors in order to balance air traffic controller (ATCO) workload and relieve congestion in voice communication. Airspace capacity has traditionally been defined as the maximum traffic that can be controlled under acceptable workload levels[1]. Each sector has a capacity limit, or sector capacity, defined by the maximum number of aircraft that can be handled in the sector during a given time period[2]. Given the strong influence of ATCO workload, sector capacity is in turn influenced by many factors relevant to workload including sector size, number of routes, number of intersections of routes, traffic volume, spatial and temporal distribution of air traffic, availability of radar control and proficiency of ATCOs.

It has been argued that with the relevant quantifiable data, dynamic density which includes both traffic density (a count of aircraft in a volume of airspace) and traffic complexity (a measure of the complexity of the air traffic in a volume of airspace), and proposed as an air traffic management metric[3], can describe the sector complexity precisely. Research on dynamic density

* Corresponding author, E-mail address: minghuahu@nuaa.edu.cn.

How to cite this article: Dong Xiangning, Hu minghua, Washington Yotto Ochieng. Sector capacity estimation based on differentiated routes and busy levels[J]. Trans. Nanjing Univ. Aero. Astro., 2017,34(4):438-448.
http://dx.doi.org/10.16356/j.1005-1120.2017.04.438

and complexity has focused on some parameters such as sector aircraft count, monitor alert parameter (MAP), sector volume, and speed change that could enable traffic flow management personnel to strategically prevent overloads using triggers other than predicted sector traffic count[4]. Christien el al. built an adapted macroscopic workload model to identify groups of sectors sharing similar complexity indicators levels[5].

Fundamentally, sector capacity is closely linked to the air traffic flows and sector structure[6]. Furthermore, it has been shown that ATCO workload is highly correlated with sector structure[7]. Welch et al. introduced a macroscopic capacity model that accounts for workload from conflict avoidance tasks[8]. However, ATCO workload is generated by other tasks in addition to conflict resolution. Lee et al. introduced a complexity map to describe airspace complexity by capturing how difficult a given traffic situation is in terms of the control activities required to accommodate disturbances such as the entrance of another aircraft into the airspace. However, they considered only the horizontal motion of aircraft, neglecting vertical motion. The 79 controllers were interviewed from 14 area control centers in Europe, Asia and Africa to capture the factors that influence their workload[9]. On the basis of these interviews, a taxonomy of more than 50 complexity variables subdivided into 11 major groupings, such as traffic mix and entry and exit points, was developed. Such taxonomy could assist airspace planners to design sectors that avoid complex air traffic control (ATC) situations. Majumadar et al. also carried out a simulation study for the Central European Air Traffic Services (CEATS) Upper Area Control Centre region of Europe[10]. The work showed that en-route sector capacity can be estimated based on ATCO workload. For terminal airspace, Netjasov et al. developed a generic metric for measuring complexity[11]. Bazargan et al. used total airport and airspace model (TAAM) to estimate Philadelphia International Airport (PHL) runway capacity[12]. Because of the very high level of detail and closely representing reality in terms of applicable separation standards and air traffic control procedures, it is a very complicated and time-consuming work to construct a TAAM model.

From the review above, most workload (and hence capacity) estimation methods have been developed for the en-route airspace or area control environment, with a few developed for the approach control environment. Therefore, firstly, there is a need for one method that applies to both area and approach control sectors. Secondly, the current methods are designed for either simulated or real ATC environments. There is therefore, a further requirement for the generic method to be applicable to both simulated and real environments. Finally, previous research developed ATCO workload model from different perspectives and principles, integration is difficult and may not be optimal. The combination of different routes and busy levels is a simple way of capturing sector complexity and its relationship to ATCO workload and hence sector capacity.

This paper proposes a simple common workload-based en-route and approach sector capacity estimation method applicable with simulated or real workload data. Cognitive complexity is a limiting factor on the capacity and efficiency of the ATC system, and the concept of structure-based abstractions such as standard flows is shown to be useful tools for ATCOs to identify cognitive complexity[13]. In this paper, it is assumed that the workload of controlling one flight along the same route in a sector is the same under the same busy level. Therefore, the workload of one flight along the same route under the same busy level is captured over time, and the mean value taken to represent the workload of a specified route and busy level. The choice of the mean value as the metric is justified by the analysis of the standard deviations, showing significantly lower values considering busy levels compared to without considering busy levels. The workload for each route and busy level over a period of time (e. g. 15 min or 1 h) is then determined by the product of the corresponding mean workload and the number of flights within that period of time. Subsequently, through regression analysis, the relationship between workload and number of flights for the 15 min and 1 h time slices is determined. The sector capacity is then calculated according to the workload threshold, which is determined by a minimum proportion of time that the ATCOs must have for recuperation if the sector is to continue to be operated safely.

Here, the model of ATCO workload is presented, as well as its method of application. The model is then applied and divided into three parts: the first part analyzes the Zhengzhou approach control airspace structure, identifies the different routes and generates the traffic flow statistics; the second part calculates the workload without considering the busy levels and generates the regression equation of ATCO workload and number of flights; the third part considers the busy levels in the computation of workload and generates the corresponding regression equation. Finally, the sector capacity values for the two scenarios are calculated. The results are analyzed and discussed.

1 Model of ATCO Workload

Safe and efficient operation of flights in airspace requires ATCOs to undertake many tasks. Both physical and mental processes are required for ATCOs to fulfill these tasks in time. Airspace factors and operational constrains are key contributors to ATCO task demand and mental workload[13,14]. Workload is a construct, i. e., a non-directly observable magnitude, necessitating the observation of related observable phenomena[15-18]. Therefore, the length of time required to execute the physical and mental tasks is a reflection of the air traffic control workload.

The workload includes communication workload, non-communication workload, and thinking (cognitive) workload. Communication workload consists of the durations of both controller and pilot transmissions. Non-communication workload is made up of the durations of non-communication such as flight progress strip processing, human machine interface (HMI) operation and coordination with others. Thinking or cognitive workload is composed of the durations of controller thinking before issuing a clearance or instruction to a pilot.

The ATCO workload can be calculated

$$WL_i(t)=\sum_{j=1}^{n}\overline{WL_{ij}}N_i(t)_j$$
$$i\in\{1,2,\cdots,l\},\quad j\in\{1,2,\cdots,n\} \tag{1}$$

where

$$\overline{WL_{ij}}=\overline{WL_i^{\mathrm{com}}}_j+\overline{WL_i^{\mathrm{non\text{-}com}}}_j+\overline{WL_i^{\mathrm{thk}}}_j \tag{2}$$

where $WL_i(t)$ is the ATCO workload of the sector in time slice t under busy level i; l the most busy level, usually taken to be 3; n the total number of routes in the sector; $\overline{WL_{ij}}$ the mean workload of controlling one flight along route j under busy level i; $N_i(t)_j$ the number of flights flying along route j under busy level i in time slice t; $\overline{WL_i^{\mathrm{com}}}_j$ the mean communication workload of controlling one flight along route j under busy level i; $\overline{WL_i^{\mathrm{non\text{-}com}}}_j$ the mean non-communication workload of controlling one flight along route j under busy level i; and $\overline{WL_i^{\mathrm{thk}}}_j$ the mean thinking workload of controlling one flight along route j under busy level i.

ATCOs need time to deliver instructions, clearances and information to pilots, and also controllers need time to monitor pilots' read-backs and requests. Communication workload consists of the controller's transmitting and monitoring of the pilots' transmission in Eq. (3)

$$\overline{WL_i^{\mathrm{com}}}_j=\overline{WL_i^{\mathrm{trans}}}_j+\overline{WL_i^{\mathrm{monit}}}_j \tag{3}$$

where $\overline{WL_i^{\text{trans}}}_j$ denotes the mean controller′s transmission workload of controlling one flight along route j under busy level i; and $\overline{WL_i^{\text{monit}}}_j$ the mean controller′s monitoring workload of controlling one flight along route j under busy level i.

Non-communication workload can be calculated

$$\overline{WL_i^{\text{non-com}}}_j = \overline{WL_i^{\text{str}}}_j + \overline{WL_i^{\text{HMI}}}_j + \overline{WL_i^{\text{co}}}_j \quad (4)$$

where $\overline{WL_i^{\text{str}}}_j$ denotes the mean workload of flight progress strip processing for one flight along route j under busy level i; $\overline{WL_i^{\text{HMI}}}_j$ the mean workload of HMI processing for one flight along route j under busy level i; and $\overline{WL_i^{\text{co}}}_j$ the mean workload of coordination for one flight along route j under busy level i.

The communication and non-communication workload can be observed and recorded when ATCOs are doing their jobs either in a real operational environment or in a simulation environment. Nevertheless, the thinking workload of controlling a flight is a construct, i. e. , it cannot be observed directly. ATCOs use mainly three types of instructions, heading, level and speed changes for conflict resolution and efficient expedition of traffic through a sector. Before issuing an instruction, ATCOs need some time to think about it, i. e. , thinking workload.

The thinking workload is quantified through questionnaires completed by ATCOs. The questionnaires were designed to capture the elements of Eq. (5). For objectivity and statistical representation (and accounting for the difficulty of access to controllers), usually ten ATCOs from different working groups were selected to complete the questionnaire. The requirements were that the ATCOs should have a valid ATC license and be qualified for working in the evaluating sector. The initial design of the questionnaire was discussed with the sector supervisor and if necessary modifications could be made. Before completing the questionnaires, the ATCOs were briefed to ensure a comprehensive understanding of the content. After the questionnaires were completed, they were collected. The data were pre-processed to remove outliers based on a distribution analysis of the responses using histogram. A sample questionnaire is shown in Appendix A.

The thinking workload is expressed e in Eq. (5) as follows

$$\overline{WL_i^{\text{thk}}}_j = \overline{wl_i^{\text{heading\_thk}}}_j m_i^{\text{heading}}{}_j + \overline{wl_i^{\text{level\_thk}}}_j m_i^{\text{level}}{}_j + \overline{wl_i^{\text{speed\_thk}}}_j m_i^{\text{speed}}{}_j \quad (5)$$

where $\overline{wl_i^{\text{heading\_thk}}}_j$ denotes the mean thinking workload of a single heading instruction for one flight along route j under busy level i; $m_i^{\text{heading}}{}_j$ the mean number of heading instructions for one flight along route j under busy level i; $\overline{wl_i^{\text{level\_thk}}}_j$ the mean thinking workload of a single level instruction for one flight along route j under busy level i; $m_i^{\text{level}}{}_j$ the mean number of level instructions for one flight along route j under busy level i; $\overline{wl_i^{\text{speed\_thk}}}_j$ the mean thinking workload of a single speed instruction for one flight along route j under busy level i; $m_i^{\text{speed}}{}_j$ the mean number of speed instructions for one flight along route j under busy level i.

The number of flights along route j under busy level i in time slice t ($N_i(t)_j$) can be determined from the flight flow statistical module.

2 Applying Workload Model

The implementation of the workload model in the ZHCC AP control sector is discussed and the capacity of the sector is calculated.

2.1 ZHCC AP routes and traffic flow analysis

2.1.1 ZHCC AP routes

As shown in Fig. 1, the horizontal range or coverage of ZHCC AP is a convex polygon within the dashed lines.

The vertical coverage of ZHCC AP is from flight level 5 700 m and below, excluding the ZHCC tower control zone. There are seven different routes (i. e. , R_1 through R_7) in ZHCC AP.

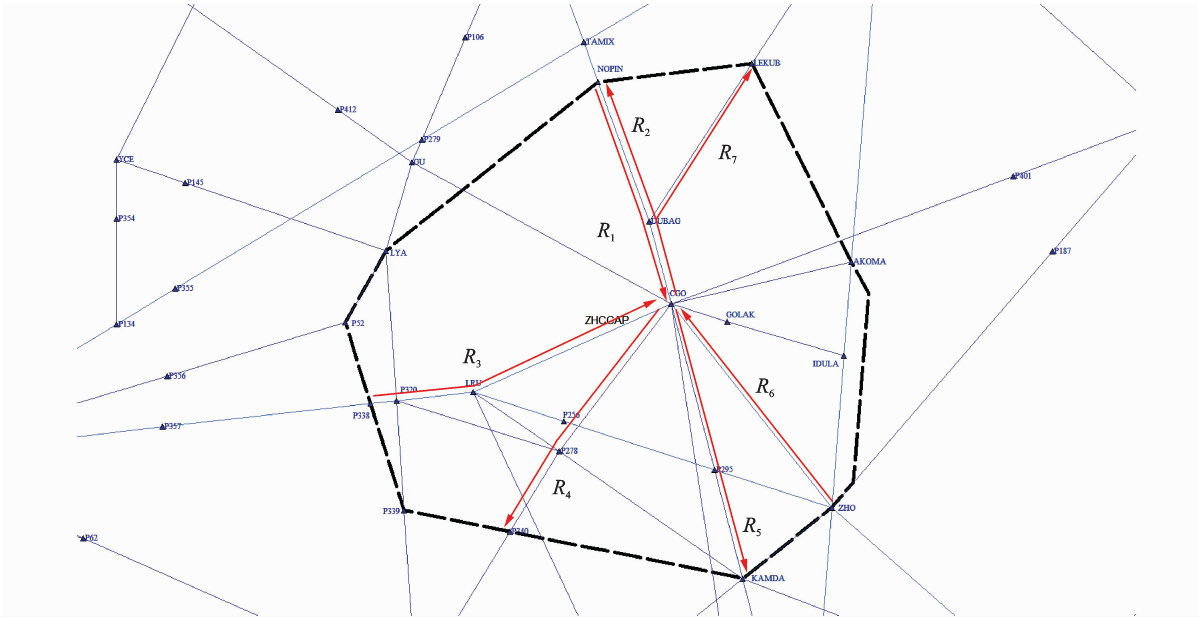

Fig. 1 Structure and routes of ZHCC AP

2.1.2 ZHCC AP traffic flow analysis

The flight data for 8 April 2014 are chosen to represent a typical busy day with no adverse weather conditions in 24 h. The seven routes (designated R_1 through R_7) with different traffic flow proportions are shown in Table 1. R_5 (KAMDA-outbound) and R_6 (ZHO-inbound) are the busiest routes in ZHCC AP.

Table 1 Traffic flow proportions for 7 routes in ZHCC AP

Route ID	Route description	Traffic flow proportion/%
R_1	NOPIN-inbound	10.91
R_2	NOPIN-outbound	2.86
R_3	P338-inbound	12.73
R_4	P340-outbound	13.51
R_5	KAMDA-outbound	26.75
R_6	ZHO-inbound	24.68
R_7	LEKUB-outbound	8.56

We choose sector capacity based on the time slice of one hour and fifteen minutes. One hour capacity is in line with the conventional definition of the relationship between workload and sector capacity. However, in the ZHCC AP, the average dwelling time of flights is approximately 15 min. Therefore, it is practical to base capacity estimation over 15 min duration as representing to determine the maximum number of flights that ATCOs can handle simultaneously in this specific sector, ZHCC AP. Figs. 2, 3 show the number of flights flown in the ZHCC AP every one hour and fifteen minutes on 8 April 2014, respectively.

As shown in Figs. 2, 3, the busiest period in

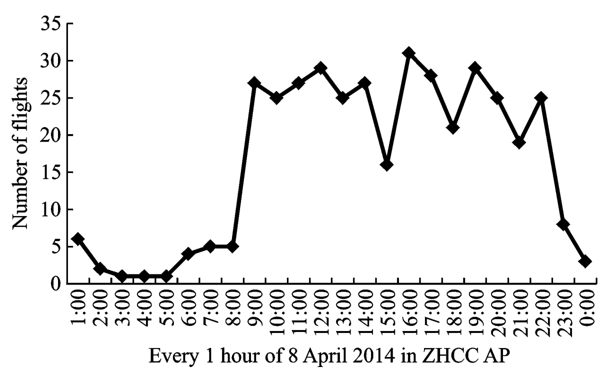

Fig. 2 Number of flights flown in ZHCC AP every 1 hour on 8 April 2014

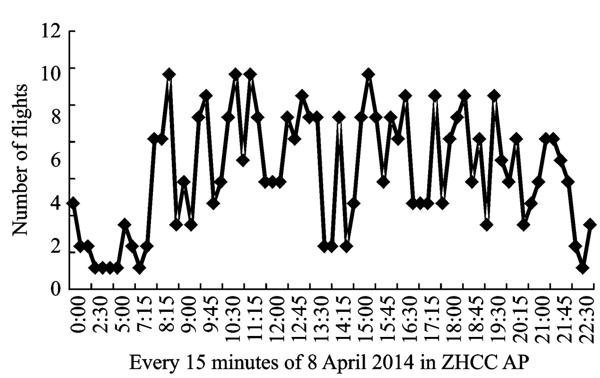

Fig. 3 Number of flights flown in ZHCC AP every 15 minutes on 8 April 2014

the ZHCC AP on 8 April 2014 was from 9:00 to 22:00 with the highest number of flights (31) per hour between 16:00 and 17:00. The corresponding number per 15 min of 10 flights occurred four times on that day.

2.2 Scenario A: Without consideration of busy levels

2.2.1 ATCO workload calculation

In order to compare the two capacity estimations for the two scenarios without and with the consideration of busy levels, the corresponding workloads are calculated in the first instance. Firstly, without considering busy levels, the mean communication, non-communication and thinking workloads and the mean overall workload per flight and their standard deviations (SD) are listed in Table 2.

As shown in Table 2, the ATCO workloads for flights on routes R_1, R_2, R_3 and R_6 are almost double those on routes R_4, R_5 and R_7. It is shown that the communication workloads for flights on routes R_1, R_2, R_3 and R_6 are significantly higher than those on routes R_4, R_5 and R_7. Hence, it can be concluded that communication workload is the main component of the ATCO workload in the ZHCC AP. Also, the thinking workload for flights on routes R_2, R_4, R_5 and R_7 are less than those on routes R_1, R_3 and R_6. The main reason for this is that ATCO thinking workload is higher for inbound flights than outbound flights.

Table 2 Scenario A: Mean and SD values of workload per flight of different routes s

Route ID	Communication workload mean value/SD value	Non-communication workload mean value/SD value	Thinking workload mean value/SD value	Overall workload mean value/SD value
R_1	31.15/14.96	16.06/4.05	14.33/5.59	61.54/18.63
R_2	28.92/2.65	15.50/0.50	9.20/4.09	53.62/2.15
R_3	25.66/6.62	15.25/2.45	13.93/5.30	54.84/9.04
R_4	11.25/2.76	6.60/0.80	10.27/4.12	28.12/3.51
R_5	13.08/6.88	7.00/0.82	8.87/3.34	28.95/7.66
R_6	32.42/10.91	20.26/3.60	14.73/4.88	67.41/14.06
R_7	16.85/1.64	5.50/0.50	6.80/3.75	29.15/2.14

From Table 2, the three overall workload values, i.e., mean, upper bound and lower bound value are determined.

2.2.2 Regression analysis of ATCO workload and number of flights

In scenario A (without consideration of busy levels), Figs. 4, 5 show the regressions of ATCO workload (workload value per flight times number of flights) and number of flights in 1 h and in 15 min, respectively.

In Fig. 4, the abscissa of the flight numbers-workload curve is the number of flights controlled within the ZHCC AP sector per hour, and the ordinate is the correspondent ATC workload. The blue diamond dots represent the upper bound workload, the red square dots represent the mean workload and the green triangle dots represent the lower bound workload. Quadratic polynomial regression is chosen and the nodal increment is set to be 5% of 1 hour, i.e., 180 s. The nodal increment is set because controllers believe that even

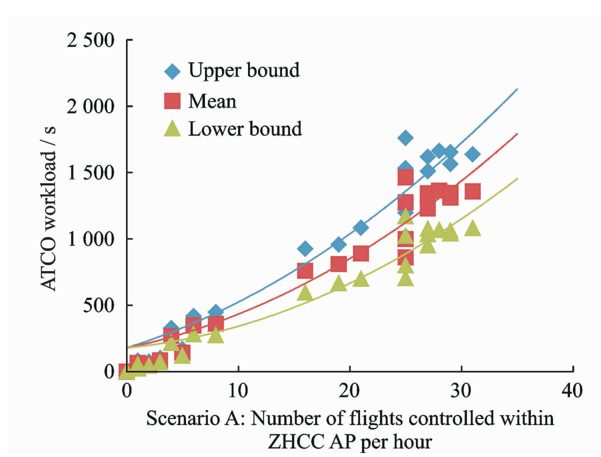

Fig. 4 Scenario A: Regression of workload and number of flights (1 h)

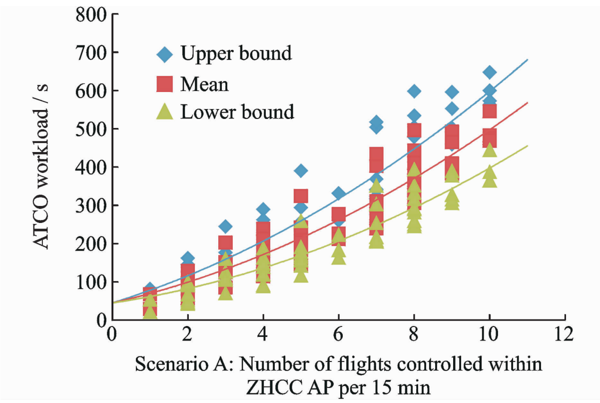

Fig. 5 Scenario A: Regression of workload and number of flights (15 min)

when there is no aircraft in the sector, they still need to keep the headset on and monitor the radar screen. So the nodal increment is set as the base of the ATC workload, set to 5% following discussion with the sector supervisor.

There are three curves in Fig. 4, i. e., blue (upper bound), red (mean) and green (lower bound) best-fit regression lines and their regression equations are shown below as Eqs. (6)—(8), respectively

$$WL_{A:\mathrm{up\_1hr}}=0.852\,6N^2+25.834N+180 \quad (6)$$

$$WL_{A:\mathrm{mn\_1hr}}=0.829\,1N^2+17.006N+180 \quad (7)$$

$$WL_{A:\mathrm{lb\_1hr}}=0.805\,6N^2+8.1762N+180 \quad (8)$$

The coefficients of determination (R-squared values) of the three equations are 0.942 3, 0.936 1 and 0.922 3, respectively.

Similarly, the nodal increment is set to be 5% of 15 min, i. e., 45 s. There are three curves for 15 min time slice shown in Fig. 5 with the corresponding regression equations are shown below as Eqs. (9)—(11), respectively.

$$WL_{A:\mathrm{up\_15min}}=2.479\,2N^2+30.453N+45 \quad (9)$$

$$WL_{A:\mathrm{mn\_15min}}=2.273\,8N^2+22.49N+45 \quad (10)$$

$$WL_{A:\mathrm{lb\_15min}}=2.068\,4N^2+14.523N+45 \quad (11)$$

The coefficients of determination (R-squared values) of the three equations are 0.881 2, 0.882 7 and 0.879 1, respectively.

Although the R-squared values of 15 min, i. e., 0.881 2, 0.882 7 and 0.879 1 are less than the value of 1 hour, i. e., 0.942 3, 0.936 1 and 0.922 3, it should be noted that there is less data for the 1 h slices than for the 15 min slices. The six R-squared values are high and each demonstrates a good fit.

2.3 Scenario B: with busy level consideration

2.3.1 ATCO workload calculation

For three busy levels, the mean communication, non-communication and thinking workload are calculated and added up to determine the mean overall workload, as shown in Table 3. As the number of flights in a given day fluctuates, three busy levels (I, II, III) are defined. Level I is when the number of flights in 1 hour or 15 minutes is below 30% of the highest number of flights in 1 hour or 15 minutes. Similarly, 31% to 70% is Level II and above 70% is Level III.

Table 3 Scenario B: mean and SD values of overall workload per flight of different routes s

Route ID		R_1	R_2	R_3	R_4	R_5	R_6	R_7
Communication workload mean value/SD value	Busy level I	15.82/7.15	28.92/0	17.59/2.36	9.03/0.38	6.55/0	22.35/4.92	16.85/0
	Busy level II	29.86/1.86	28.92/0	29.28/1.83	10.86/0.02	10.09/0	36.01/4.75	16.85/0
	Busy level III	47.46/7.73	28.92/0	32.33/0.62	16.50/0	22.59/0	48.76/1.92	16.85/0
Non-communication workload mean value/SD value	Busy level I	11.08/1.79	15.50/0	12.42/0.94	6.00/0	6.00/0	17.09/1.58	5.50/0
	Busy level II	18.00/1.25	15.50/0	16.08/0.47	6.50/0.5	7.00/0	21.54/2.48	5.50/0
	Busy level III	19.58/0.83	15.50/0	18.25/0.62	8.00/0	8.00/0	25.04/1.91	5.50/0
Thinking workload mean value/ SD value	Busy level I	8.60/1.85	4.80/0.98	8.00/2.61	5.80/1.60	6.00/1.26	17.09/1.94	5.50/1.60
	Busy level II	13.00/2.28	8.60/1.02	13.60/1.20	10.40/2.06	8.40/2.33	14.40/1.36	6.40/2.94
	Busy level III	21.40/0.80	14.20/1.83	20.20/1.17	14.60/2.33	12.20/2.63	20.60/0.80	10.20/.3.19
Overall workload mean value/ SD value	Busy level I	35.50/8.79	49.22/0.00	38.01/3.30	20.83/0.38	18.55/1.36	48.04/6.26	26.15/3.26
	Busy level II	60.85/2.23	53.02/0.00	58.96/2.27	27.76/0.52	25.49/3.87	71.95/5.34	28.75/3.15
	Busy level III	88.45/8.22	58.62/0.00	70.78/1.12	39.10/0.00	42.79/8.03	94.41/1.50	32.55/4.13

As shown in Table 3, the overall workload per flight increases with the increase of busy levels in all routes. The fact that R_1, R_3, R_4, R_5 and R_6 increase more than R_2 and R_7 shows that the former 5 routes become more complex than the latter 2 routes when more flights are added to that route. There are four times that the overall workload SD value is 0.00. The reason for this is due to the limited time of field observation. For example, there was only one sample for R_2 under each of the three busy levels and for R_4 under busy level III. Fortunately, for all the routes and busy levels, 48 samples were collected considered adequate for regression analysis.

2.3.2 Regression analysis of ATCO workload and number of flights

For scenario B (considering busy levels), Figs. 6, 7 show the regressions of ATCO workload and the number of flights in 1 h and 15 min, respectively.

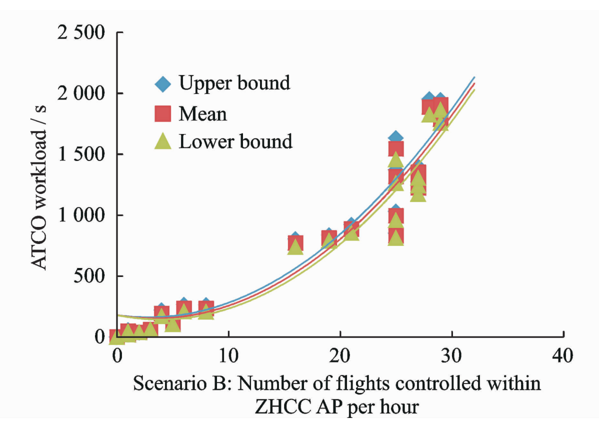

Fig. 6 Scenario B: Regression equation of workload and number of flights (1 h)

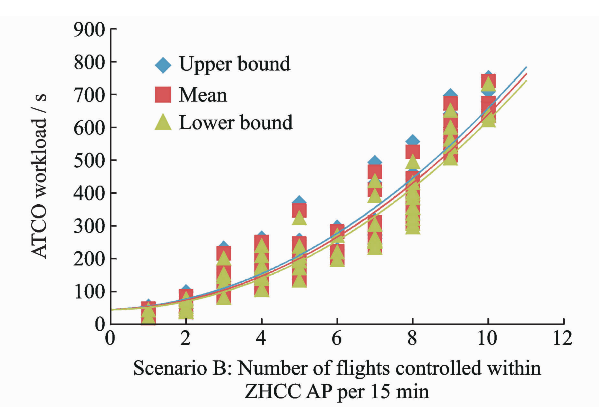

Fig. 7 Scenario B: Regression equation of workload and number of flights (15 min)

As mentioned in Section 2.2.2, quadratic polynomial regression is chosen and the nodal increment is set to be 5% of 1 h and 15 min, i.e., 180 s and 45 s, respectively. There are three curves both in Figs. 6, 7, i.e., blue (upper bound), red (mean) and green (lower bound) best-fit regression lines and their regression equations are shown below as Eq. (12), Eq. (13) and Eq. (14) for 1 h and Eq. (15), Eq. (16) and Eq. (17) for 15 min, respectively

$$WL_{B:\text{ub\_1hr}} = 2.309\,8N^2 - 12.941N + 180 \tag{12}$$

$$WL_{B:\text{mn\_1hr}} = 2.349\,1N^2 - 15.789N + 180 \tag{13}$$

$$WL_{B:\text{lb\_1hr}} = 2.383N^2 - 18.494N + 180 \tag{14}$$

$$WL_{B:\text{ub\_15min}} = 5.667\,1N^2 + 2.908\,2N + 45 \tag{15}$$

$$WL_{B:\text{mn\_15min}} = 5.669\,2N^2 + 2.908\,2N + 45 \tag{16}$$

$$WL_{B:\text{lb\_15min}} = 5.665\,4N^2 + 1.055\,7N + 45 \tag{17}$$

The coefficients of determination (R-squared values) of the six equations are 0.922 2, 0.923 4, 0.923 9, 0.876 4, 0.884 5 and 0.891 5, respectively. They are all acceptably high and each demonstrates a good fit.

From the results, the general trend is that ATCO workload increases with the number of flights. However, the results in Figs. 4, 5 showing that ATCO workload increases almost linearly (i.e. the coefficients for the second order parameter is relatively small compared to those with busy level consideration case) with the number of flights, which is not realistic, mainly due the averaging effect over the periods considered in addition to non-consideration of the busy levels. When an ATCO is busy with controlling flights, the addition of a single flight should result in more workload compared to that for controlling one flight when not busy. This effect is captured in Figs. 6, 7, with a non-linear relationship between the number of flights and workload.

Comparing scenario A of Figs. 4, 5 and scenario B of Figs. 6, 7, the differences among upper bound workload, mean workload and lower bound workload in scenario A are bigger than those in scenario B. This means that workload data is better represented with busy levels consideration than the one without.

3 Sector Capacity Estimation

The capacity values without (Scenario A) and with (Scenario B) busy levels are calculated in this section.

3.1 Workload threshold

According to the International Civil Aviation Organization (ICAO), the average workload at capacity must be less than 80% and workload of 90% must not be exceeded more than 2.5% of the time[19]. Table 4 presents the threshold values and their qualitative interpretation from validated real time simulation studies and operational trials by Eurocontrol[20].

Table 4 Threshold values of workload in Europe

Threshold	Interpretation	Recorded working time during 1 h
70% or above	Overload	42 min
54%—69%	Heavy load	32—41 min
30%—53%	Medium load	18—31 min
18%—29%	Light load	11—17 min
0%—17%	Very light load	0—10 min

To find a compromise between safety and efficiency, 65% of 1 h (i.e. 2 340 s) and 80% of 15 min (i.e. 720 s) are chosen in this paper to be the threshold values of workload.

3.2 Computation of sector

The threshold values are substituted in the regression equations in Figs. 4—7 as WL and the nonnegative real number N is solved. Consequently, the rounded off integers of N are considered to be the capacity values, as shown in Table 5.

In Table 5, it can be seen that the capacity value for scenario A has a higher spread than scenario B both for 1 h and for 15 min periods. Furthermore, compared to the actual peak traffic volume figures of 31 and 10, it is concluded that the consideration of busy levels results in higher precision and accuracy of sector capacity estimation.

Table 5 Capacity values of ZHCC AP

Scenario	Workload	Capacity values for 1 h	Capacity values for 15 min
A	Upper bound	37	11
	Mean	41	12
	Lower bound	46	14
B	Upper bound	33	10
	Mean	33	10
	Lower bound	34	10

4 Discussion

The capacity values for 1 h and 15 min time slices in scenario A are higher than in scenario B reflecting the uncertainty of the model without considering of busy levels, as shown by the relatively large spread (i. e. standard deviation) in Figs. 4, 5. On the contrast, the relatively narrow spread (standard deviation) in Figs. 6, 7 reflect the high degree of certainty. Furthermore, the capacity value for the 1 hour period is 41 in scenario A, much higher than 32 in scenario B while the capacity value for the 15 minutes period in scenario A is 12, not very high compared to 10 for scenario B. It is notable that the capacity value for 15 min period is higher a quarter of that for 1 h period. This is because ATCOs can sustain high workload or even overload for a short time period, for example 15 min, but cannot sustain this for a long period, such as 1 h. However, the main reason for the differences is that the relationship of ATCO workload and number of flights is not linear. As the number of flights increases, there is the potential for more conflicts with a corresponding increase in the mean workload for controlling a given flight. Therefore, in order to more accurately represent the variation in the workload according to the change in number of flights, three different busy levels (scenario B) are introduced here.

It is found that the consideration of busy levels results in a more realistic and accurate determination of capacity in line with ATCO experiences. The peak numbers of flights in Figs. 2 and 3, 31 and 10, respectively, are very close to the capacity values of 33 and 10 for the 1 h and 15 min periods, respectively for scenario B.

From Figs. 2, 3 and based on the estimated capacity values in this paper, it can be seen that there are periods when the number of flights in the ZHCC AP sector approaches the maximum capacity. As a result and in order to prevent controller overload and the potential consequences, in 2015 the ZHCC AP sector authorities divided vertically the original approach airspace into two parts referred to as the high sector and low sector. The two new sectors went into operation on 7th January 2016.

5 Conclusions

This paper has presented a generic method for sector capacity estimation based on ATCO workload. Unlike the current methods of capacity estimation based on workload which are designed for use in either area control or approach control sectors, the method developed in this paper is generic. The three main parts of workload, i. e., communication, non-communication and thinking (or cognitive) workload is substituted in the proposed workload model considering differentiated routes and busy levels. The relationship between workload and the number of flights in a given time period is determined through regression analysis. Sector capacity is then determined on the basis of a specified workload threshold. The results show that with the proposed workload model considering differentiated routes and busy levels, both approach control and area control sector capacity values can be estimated with a high degree of precision and accuracy. It is recommended that the proposed model can be used by air traffic service providers for sector capacity evaluation.

Acknowledgments

This work was partially supported by the National Natural Science Foundation of China (No. 61304190) and the Fundamental Research Funds for the Central Universities (No. NJ20140018).

References:

[1] MAJUMDAR A, OCHIENG W, POLAK J. Estimation of european airspace capacity from a model of controller workload[J]. Journal of Navigation, 2002, 55(3): 381-403.

[2] LEE K, FERON E, PRITCHETT A. Describing airspace complexity: Airspace response to disturbances[J]. Journal of Guidance Control & Dynamics, 2008, 32(1): 210-222.

[3] LAUDEMAN L V, SHELDEN S G, BRANSTROM R, et al. Dynamic density: An air traffic management metric: NASA TM-1998-112226[R]. Moffett Field, CA, USA: NASA Ames Research Center, 1998: 1-15.

[4] MASALONIS A J, CALLAHAM M B, WANKE C R, et al. Dynamic density and complexity metrics for realtime traffic flow management[R]. McLean, VA, USA: MITRE, 2003: 1-10.

[5] CHRISTIEN R, BENKOUAR A. Air traffic complexity indicators & ATC sectors classification[C]// 5th USA/Europe Air Traffic Management R&D Seminar. Budapest, Hungary: [s. n.], 2003: 1-8.

[6] CHATTERJI G, ZHENG Y, KOPARDEKAR P. Analysis of current sectors based on traffic and geometry: AIAA Paper 2008-7227[R]. Honolulu, Hawaii, USA: AIAA Guidance, Navigation, and Control Conference and Exhibit, 2008.

[7] SHERALI H D, HILL J M. Configuration of airspace sectors for balancing air traffic controller workload[J]. Annals of Operations Research, 2013, 203: 3-31.

[8] WELCH J D, ANDREWS J W. Macroscopic capacity model with individual sector closing speed estimates[C]// 9th Aviation Technology, Integration, and Operations Conference (ATIO). USA: AIAA, 2009:1-11.

[9] MAJUMDAR A, OCHIENG W. Air traffic control

complexity and safety: Framework for sector design based on controller interviews of complexity factors [J]. Journal of the Transportation Research Board, 2007(1):70-80.

[10] MAJUMDAR A, OCHIENG W, MCAULEY G, et al. The factors affecting airspace capacity in europe: A cross-sectional time-series analysis using simulated controller workload data[J]. Journal of Navigation, 2004, 57(3):385-405.

[11] NETJASOV F, JANIC M, TOSIC V. Developing a generic metric of terminal airspace traffic complexity [J]. Transportmetrica, 2011, 7(5):369-394.

[12] BAZARGAN M, FLEMING, K, SUBRAMANIAN P. A simulation study to investigate runway capacity using TAAM[C]// Proceedings of the 2002 Winter Simulation Conference. San Diego, California, USA: [s. n.], 2002.

[13] HISTON J M, HANSMAN R J. Mitigating complexity in air traffic control: The role of structure-based abstractions: Report No. ICAT-2008-05[R]. Cambridge, MA: Massachusetts Institute of Technology, 2008.

[14] LOFT S, SANDERSON P, NEAL A, et al. Modeling and predicting mental workload in en route air traffic control: Critical review and broader implications[J]. Human Factors, 2007, 49(3):376-399.

[15] WILLIAM S P, CHRISTOPHER R B, Kimberly C. et al. A framework for the evaluation of air traffic control complexity: AIAA Paper 96-3856[R]. San Diego, CA, USA: AIAA, Guidance, Navigation and Control Conference, 1996.

[16] TOBARUELA G, SCHUSTER W, MAJUMDAR A, et al. A method to estimate air traffic controller mental workload based on traffic clearances[J]. Journal of Air Transport Management, 2014, 39:59-71.

[17] WANG Y, BU J, HAN K, et al. A novel network approach to study communication activities of air traffic controllers[J]. Transportation Research Part C Emerging Technologies, 2016, 68:369-388.

[18] WANG Y, VORMER F, HU M, et al. Empirical analysis of air traffic controller dynamics[J]. Transportation Research Part C Emerging Technologies, 2013, 33(4):203-213.

[19] International Civil Aviation Organization (ICAO). Doc 9426-AN/924, Air Traffic Service Planning Manual[S]. Montreal: ICAO, 1984.

[20] EUROCONTROL. Pessimistic sector capacity estimation: EEC Note No. 21/03[R]. 2003.

Mr. **Dong Xiangning** is currently a Ph. D. candidate and a lecturer in College of Civil Aviation at Nanjing University of Aeronautics and Astronautics (NUAA). He received his B. S and M. S. degree in Traffic Transportation Planning and Management from NUAA, in 1997 and 2006, respectively. From 1997 to present, he works as a college teacher in College of Civil Aviation, NUAA. His research interests are airspace management and capacity estimation.

Prof. **Hu Minghua** is currently a professor and doctoral supervisor at NUAA. He is the director of National Key Laboratory of Air Traffic Flow Management of China. His research interests are air traffic flow management and airspace management.

Prof. **Washington Yotto Ochieng** is the Head of the Centre for Transport Studies and Chair in Positioning and Navigation Systems at Imperial College London. In 2013, Professor Ochieng was elected Fellow of the Royal Academy of Engineering (FREng) in recognition of his exceptional contribution to engineering. He holds a PhD degree in Civil Engineering (Space Geodesy) from the University of Nottingham. He is a Chartered Engineer and Fellow of the UK Institutions of Civil Engineers, Chartered Institution of Highways and Transportation, Royal Institute of Navigation and Chartered Institution of Civil Engineering Surveyors. Professor Ochieng's research and development interests are in positioning and navigation, geospatial/geomatic engineering, Air Traffic Management (ATM) and Intelligent Transport Systems (ITS). He has made significant contributions to major international projects including the design of the European Geostationary Navigation Overlay Service (EGNOS) and GALILEO, GNSS measurement error modelling, specification of aircraft trajectory management tools for the Single European Sky's ATM Research (SESAR) program, and integrated positioning and navigation systems for many applications including ITS.

(Executive Editor: Zhang Tong)